AD-A176 339 ON PROTON BOMBARDMENT OF SILICON SEMICONDUCTORS IONIZATION VS DISPLACEMEN (U) R AND D ASSOCIATES MARINA DEL REY CA G M SAFONOV ET AL. 01 FEB 85 RDA-TR-135610-001 DNA-TR-85-262 1/1

UNCLASSIFIED F/G 9/1 NL

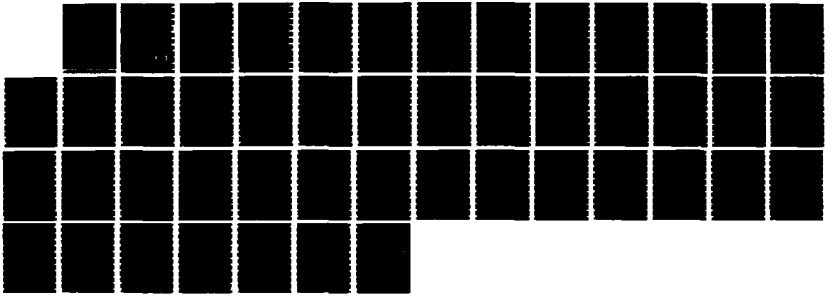

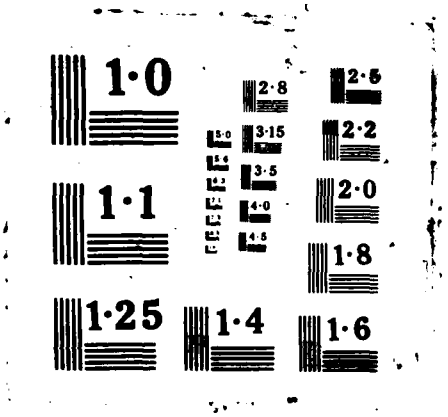
1·0
1·1
1·25
2·8
3·15
3·5
4·0
4·5
2·5
2·2
2·0
1·8
1·4
1·6

(12)

DNA-TR-85-262

ON PROTON BOMBARDMENT OF SILICON SEMICONDUCTORS

Ionization vs Displacement Disablements

George M. Safonov
Ernest A. Martinelli
George C. Messenger
R&D Associates
P. O. Box 9695
Marina del Rey, CA 90295

1 February 1985

Technical Report

CONTRACT No. DNA 001-85-C-0022

THIS WORK WAS SPONSORED BY THE DEFENSE NUCLEAR AGENCY
UNDER RDT&E RMSS CODE B310085466 P99QMXDB00099 H2590D.

Prepared for
Director
DEFENSE NUCLEAR AGENCY
Washington, DC 20305-1000

Destroy this report when it is no longer needed. Do not return to sender.

PLEASE NOTIFY THE DEFENSE NUCLEAR AGENCY, ATTN: STTI, WASHINGTON, DC 20305-1000, IF YOUR ADDRESS IS INCORRECT, IF YOU WISH IT DELETED FROM THE DISTRIBUTION LIST, OR IF THE ADDRESSEE IS NO LONGER EMPLOYED BY YOUR ORGANIZATION.

UNCLASSIFIED

SECURITY CLASSIFICATION OF THIS PAGE AD-A176337

REPORT DOCUMENTATION PAGE

Form Approved
OMB No 0704-0188
Exp Date Jun 30, 1986

1a REPORT SECURITY CLASSIFICATION UNCLASSIFIED	1b RESTRICTIVE MARKINGS
2a SECURITY CLASSIFICATION AUTHORITY N/A since Unclassified	3 DISTRIBUTION/AVAILABILITY OF REPORT Approved for public release; distribution is unlimited.
2b DECLASSIFICATION/DOWNGRADING SCHEDULE N/A since Unclassified	
4 PERFORMING ORGANIZATION REPORT NUMBER(S) RDA-TR-135610-001	5 MONITORING ORGANIZATION REPORT NUMBER(S) DNA-TR-85-262
6a NAME OF PERFORMING ORGANIZATION R & D Associates 6b OFFICE SYMBOL (If applicable)	7a NAME OF MONITORING ORGANIZATION Director Defense Nuclear Agency
6c ADDRESS (City, State, and ZIP Code) P. O. Box 9695 Marina del Rey, CA 90295	7b ADDRESS (City, State, and ZIP Code) Washington, DC 20305-1000
8a NAME OF FUNDING/SPONSORING ORGANIZATION 8b OFFICE SYMBOL (If applicable)	9 PROCUREMENT INSTRUMENT IDENTIFICATION NUMBER DNA 001-85-C-0022
8c ADDRESS (City, State, and ZIP Code)	10 SOURCE OF FUNDING NUMBERS PROGRAM ELEMENT NO: 62715H; PROJECT NO: P99QMXD; TASK NO: B; WORK UNIT ACCESSION NO: DH008670

11 TITLE (Include Security Classification)
ON PROTON BOMBARDMENT OF SILICON SEMICONDUCTORS
Ionization Vs Displacement Disablements

12 PERSONAL AUTHOR(S)
Safonov, George M.; Martinelli, Ernest A.; and Messenger, George C.

13a TYPE OF REPORT	13b TIME COVERED	14 DATE OF REPORT (Year, Month, Day)	15 PAGE COUNT
Technical	FROM 840801 TO 850201	850201	46

16 SUPPLEMENTARY NOTATION
This work was sponsored by the Defense Nuclear Agency under RDT&E RMSS Code B310085466 P99QMXDB00099 H2590D.

17 COSATI CODES			18 SUBJECT TERMS (Continue on reverse if necessary and identify by block number)
FIELD	GROUP	SUB-GROUP	Proton Beams; Silicon Semiconductor Targets; Ionization Damage; Straggling Effects; Displacement Damage; Semiconductor Disablement
20	07		
09	05		

19 ABSTRACT (Continue on reverse if necessary and identify by block number)

The bombardment of thick silicon-crystalline targets by monodirectional and monoenergetic beams of 25 to 250 MeV protons is considered. By use of a proton-fluence model that accounts for straggling effects, total ionization dose and silicon-atom displacement-density profiles within the target material are determined and presented as functions of incident particle energy. For assumed values of total dose [1 Mrad(Si)] and displacement [10^{14} 1-Mev-equivalent-neutrons/cm^2] levels that would disable typical semiconductors, the times required for a beam of "reference" proton flux [10^{13} protons/cm^2·s] to disable such devices by each of the two mechanisms are computed. Profiles of the ratio of the two disablement times are presented as functions of incident proton energy. For the reference disablement criteria, ionization disablement is found to precede displacement-disablement. Means to scale results to other values of these criteria are noted. Plans to extend the work to cover all three of the hydrogen-isotope beams are noted and the desirability of certain related experimental data is discussed. An appendix details the construction of a function assumed to represent-

20 DISTRIBUTION/AVAILABILITY OF ABSTRACT	21 ABSTRACT SECURITY CLASSIFICATION
☐ UNCLASSIFIED/UNLIMITED ☒ SAME AS RPT ☐ DTIC USERS	UNCLASSIFIED
22a NAME OF RESPONSIBLE INDIVIDUAL Betty L. Fox	22b TELEPHONE (Include Area Code) (202) 325-7042
	22c OFFICE SYMBOL DNA/STTI

DD FORM 1473, 84 MAR 83 APR edition may be used until exhausted
All other editions are obsolete

SECURITY CLASSIFICATION OF THIS PAGE
UNCLASSIFIED

19. ABSTRACT (Continued)

the displacement damage coefficient.

Accession For	
NTIS GRA&I	X
DTIC TAB	☐
Unannounced	☐
Justification	
By	
Distribution/	
Availability Codes	
Dist	Avail and/or Special
A-1	

SUMMARY

This report concerns two of the mechanisms by which high-energy protons can disable silicon semiconductors: ionization and displacement. The basic difference between these two mechanisms is fairly concisely explained in a recent text as follows:

> "Displacement effects are the changes that occur in the properties of a material when energetic (here, proton) radiation displaces (here, silicon) atoms from their normal positions in the lattice. These effects are in contrast to the ionizaton effects that are the result of orbital electrons being excited away from their parent (here, silicon) atoms by the radiation" (Ref. 1).

The reader is referred to that text for a detailed discussion of the various types of silicon device degradation that can result from proton bombardment.

Here we ask the question: If subjected to proton bombardment, would a silicon semiconductor device first fail by excessive ionization or by excessive displacement? To answer the question, we follow the usual custom of assuming that the two disabling mechanisms act independently of each other. This assumption, in turn, permits us to utilize the vast store of disablement information on various devices that has been accrued over years of gamma- and neutron-irradiation experiments (e.g., see Ref. 2). The former experiments (where displacement effects are negligible) determine total

ionization-dose failure levels, while the latter (where ionization effects are negligible) determine displacement-density failure levels.

To estimate ionization doses and displacement densities all along the tracks of penetrating protons, one of course needs at least a reasonable representation of the proton fluence as a function of both the position and energy of the projectile particles. By following the type of approach adopted by Mather and Segre in 1951 (Ref. 3), such a fluence function has been constructed and is described in Reference 4. This function permits an immediate estimate of the ionization dose along the path followed by a proton beam as its individual particles straggle to their various stopping locations in a thick silicon target.

To estimate displacement densities along the path one also needs a second function, a displacement damage coefficient which is dependent on proton energy. By use of two preliminary forms of this second function, the likely magnitudes of the displacement density that beams of 25- to 250-MeV protons might induce in thick silicon targets have been explored (Ref. 5). More recently, a third form of the displacement damage function has been constructed. As fully explained in the Appendix of this report, this third form was structured to conform with a wide assortment of available theoretical and experimental information. In the following sections, we will detail the findings that have been based on the Appendix displacement damage function and on the proton fluence model described in Reference 4.

Section 1 sets forth the total dose profiles in thick silicon targets that would result from bombardments by beams of 25- to 250-MeV protons. For beams of an incident "reference fluence" (10^{13} protons/cm^2, corresponding to a flow of 16 mA/m^2 for one second), the dose at points of proton-entry ranges from ~1/2 Mrad (250-MeV protons) to ~3 Mrad (25-MeV protons). The peak dose (that at the "Bragg peak" of the dose profile) occurs just short of the mean penetration depth. On the basis of the Reference 4 fluence model, the peak value is estimated to be 5.8 times the value at points of proton-entry into the thick target. This factor would be appreciably higher if straggling were not taken into account. Where the dose peaks, the fluence of surviving (i.e., unstopped) protons is estimated at ~81% of the incident fluence.

In Section 2, we estimate the capability of protons (at all points along their paths in the thick silicon crystal target) to cause silicon atom displacements relative to the same capability of 1-MeV neutrons.* It is customary to relate the proton-induced displacement density to that induced by 1-MeV neutrons, since the displacement-disabling fluences of such neutrons have been measured over years of nuclear weapons effects experiments. The profiles of the displacement damage ratio are presented for beams of protons with incident

*Since the spectra of neutrons from sources used in displacement damage experiments vary considerably, it has become customary to equate the fluence using a particular source spectrum to the "1-MeV-equivalent neutron fluence" that would cause the same displacement damage.

energies in the same 25- to 250-MeV range examined in our total dose study. We estimate that those proton beams that are capable of penetrating at least ~10 g/cm^2 of target material (i.e., with incident energies $\geq$ ~100 MeV) would be roughly twice as effective as 1-MeV neutrons in causing displacements near points of proton-entry. The peak of the displacement density profile would occur in the near-neighborhood of the mean stopping depth. For incident protons of 100-MeV, the peak proton-to-1-MeV-equivalent-neutron displacement damage ratio is estimated at ~5. For 250-MeV incident protons, the ratio is estimated at ~4. The peak ratio for the least energetic proton beam considered (25-MeV incident energy) is estimated at ~17. However, the mean penetration depth of this particular beam's protons would be only ~0.8 g/cm^2 of target material. These peak ratios would be considerably higher if straggling did not occur.

In Section 3, we compare the irradiation time to disable a typical bipolar device via excessive total dose to that for disablement via displacement damage. Reference kill criteria are taken at 1 Mrad(Si) for ionization dose disablement and at a displacement density equal to that resulting from exposure to 10^{14} 1-MeV neutrons/cm^2. Based on these reference kill criteria, a beam that delivers a flux of 10^{13} protons/cm^2·s to a thick assembly of such devices could always first kill each such device by ionization alone. Under the cited conditions, the devices located near the mean penetration depth of protons would fail (via ionization) in times ranging from ~0.06 seconds (25-MeV beam) to ~0.3 seconds (250-MeV beam). Devices near points of beam-entry would absorb the reference killing dose in somewhat longer times: ~0.3 seconds for the 25-MeV beam and ~2.0 seconds for the 250-MeV beam. Under

reference conditions, the time required to cause killing levels of the displacement density is estimated to be a factor of ~4 to ~12 larger than the ionization kill time.

We should here remind the reader that the ratio of ionization to-displacement kill times, of course, scales directly with the ionization dose kill criterion and inversely as the displacement kill criterion. For example, a device which fails (via displacements) upon exposure to only 10^{13} 1-MeV neutrons/cm^2 or to our reference 1-Mrad ionization dose, would experience--essentially simultaneously--a killing level of displacements and also a killing level of ionization. If this same displacement-sensitive device was so "total-dose-robust" as to require 10 Mrads for ionization disablement, it would first be killed by the displacement mechanism and, considerably later, be killed again by excessive ionization.

In Section 4, we recall our original plan to examine the bombardment of silicon semiconductors by deuterons and tritons as well as by the proton beams considered here. The desirability of experiments that would generate the type of input needed to extend our analyses to cover all three hydrogen-isotope beams is noted. Also, our plan to proceed analytically with similar studies involving the heavier isotope beams is outlined.

In the Appendix, we explain the construction of our final form of the displacement damage function.

PREFACE

The research documented here was conducted under the administrative supervision of Dr. David Gakenheimer, whose support and programmatic guidance are gratefully acknowledged.

Peter Haas had made useful suggestions, provided information or nuclear radiation effects on electronics, and had been responsible for bringing the authors together--a liaison that stimulated the present work.

RDA's Drs. J. Green and D. Washburn have constructively influenced the course of this research as have Dr. R. M. Zazworski of the Sandia National Laboratory at Albuquerque, and Dr. R. More of the Lawrence Livermore National Laboratory.

Finally, we wish to acknowledge the constant support of Mrs. F. Boyle, who has developed the machine programs used to compute the various quantities appearing in this report.

CONVERSION TABLE

(Symbols of SI units given in parentheses)

To convert from	to	Multiply by
angstrom	meters (m)	1.000 000 X E -10
atmosphere (normal)	kilo pascal (kPa)	1.013 25 X E +2
bar	kilo pascal (kPa)	1.000 000 X E +2
barn	meter^2 (m^2)	1.000 000 X E -28
British thermal unit (thermochemical)	joule (J)	1.054 350 X E +3
calorie (thermochemical)	joule (J)	4.184 000
cal (thermochemical)/cm^2	mega joule/m^2)(MJ/m^2)	4.184 000 X E -2
curie	giga becquerel (GBq)*	3.700 000 X E +1
degree (angle)	radian (rad)	1.745 329 X E -2
degree Fahrenheit	degree kelvin (K)	$t_K = (t_{\circ F} + 459.67)/1.8$
electron volt	joule (J)	1.602 19 X E -19
erg	joule (J)	1.000 000 x E -7
erg/second	watt (W)	1.000 000 X E -7
foot	meter (m)	3.048 000 x E -1
foot-pound-force	joule (J)	1.355 818
gallon (U.S. liquid)	meter^3 (m^3)	3.785 412 X E -3
inch	meter (m)	2.540 000 X E -2
jerk	joule (J)	1.000 000 X E +9
joule/kilogram (J/kg)(radiation dose absorbed)	Gray (Gy)**	1.000 000
kilotons	terajoules	4.183
kip (1000 lbf)	newton (N)	4.448 222 X E +3
kip/inch^2 (ksi)	kilo pascal (kPa)	6.894 757 X E +3
ktap	newton-second/m^2 (N-s/m^2)	1.000 000 X E +2
micron	meter (m)	1.000 000 X E -6
mil	meter (m)	2.540 000 X E -5
mile (international)	meter (m)	1.609 344 X E +3
ounce	kilogram (kg)	2.834 952 X E -2
pound-force (lbf avoirdupois)	newton (N)	4.448 222
pound-force inch	newton-meter (N•m)	1.129 848 X E -1
pound-force/inch	newton/meter (N/m)	1.751 268 X E +2
pound-force/foot^2	kilo pascal (kPa)	4.788 026 X E -2
pound-force/inch^2 (psi)	kilo pascal (kPa)	6.894 757
pound-mass (lbm avoirdupois)	kilogram (kg)	4.535 924 X E -1
pound-mass-foot^2 (moment of inertia)	kilogram-meter^2 (kg•m^2)	4.214 011 X E -2
pound-mass/foot^3	kilogram/meter^3 (kg/m^3)	1.601 846 X E +1
rad (radiation dose absorbed)	Gray (Gy)**	1.000 000 X E -2
roentgen	coulomb/kilogram (C/kg)	2.579 760 X E -4
shake	second (s)	1.000 000 X E -8
slug	kilogram (kg)	1.459 390 X E +1
torr (mm Hg, 0°C)	kilo pascal (kPa)	1.333 22 X E -1

*THE BECQUEREL (BQ) IS THE SI UNIT OF RADIOACTIVITY; 1 BQ = 1 EVENT/S.

**THE GRAY (GY) IS THE SI UNIT OF ABSORBED RADIATION.

TABLE OF CONTENTS

LIST OF ILLUSTRATIONS

SECTION 1

PROTON BEAM TO SILICON TARGET ENERGY TRANSFER VIA ATOM IONIZATION/EXCITATION MECHANISMS

Equation (11) of Reference 4 permits estimates of the energy transferred from a proton beam to a silicon target via non-nuclear interactions (i.e., via the so-called "dE/dx" mechanisms of silicon atom ionization and excitation). Reference 4 considers the irradiation of a uniform semi-infinite target by a uniform monodirectional beam whose axis is normal to the target face. The energies of the incoming beam particles are highly concentrated about an energy, E_m, which is one of the basic input quantities that define a beam/target system. A second input is R, the mean penetration depth of beam nuclei into the target material. For the proton/silicon system under study here, R is given by

$$R \cong 3.05 \times 10^{-3} \times E_m^b \ . \qquad (1)$$

Above, b = 1.74 and, with E_m in MeV, R is in units of g/cm^2. The third input is r, a dimensionless quantity that relates to the straggling of the proton stopping points in the thick silicon target. According to the model used in deriving Equation (11) of Reference 4, the standard deviation of the Gaussian distribution of the stopping depths is R/r. For protons, the model's prescription gives r = 71.4.

Figure 1 shows the estimated dE/dx dose that would be felt at points of a thick silicon target that is irradiated by beams that deliver a reference fluence of 10^{13} protons/cm^2 to the target face. To accure a total fluence of 10^{13} particles/cm^2

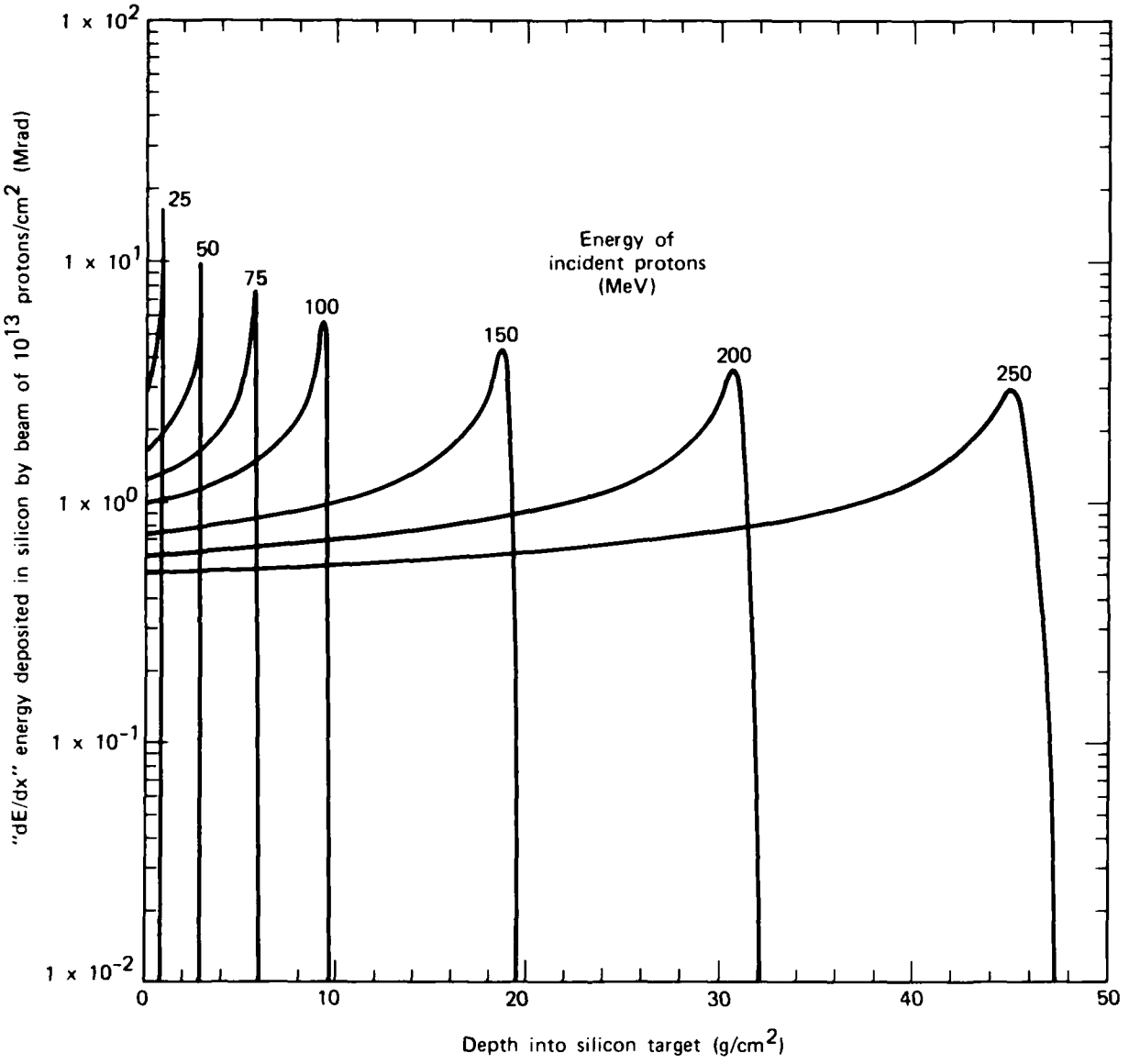

Figure 1. Energy transferred from proton beam to unit mass of silicon target via "dE/dx" mechanisms.

in one second, the average current density at the target must be 16 mA/m^2.

According to our Figure 1 estimates, a reference fluence beam of the most penetrating particles considered (i.e., 250-MeV protons) would deliver ~1/2 Mrad dose to silicon near the target face and a maximum of ~3 Mrad at the Bragg peak of the dE/dx curve. To reach silicon at depths of 10 g/cm^2 or more, proton energies above ~100 MeV would be required. And, due to the energy dependence of the dE/dx mechanisms, it is evident that the lower energy beams would be more damaging to the silicon devices within their reach than would be the more penetrating higher energy beams of equal fluence. The peak value dose is a factor of 5.8 higher than the near-surface dose according to the Reference 5 model which accounts for straggling. This factor would be significantly higher if straggling--which, of course, does occur--did not occur.

SECTION 2

SILICON ATOM DISPLACEMENT DENSITIES: PROTON-INDUCED RELATIVE TO 1-MeV-NEUTRON-INDUCED DENSITIES

The energy transferred from protons to silicon atoms via the dE/dx mechanisms has been estimated by us to be some three orders of magnitude larger than that given over to displacing these atoms from their normal positions in the silicon crystal lattice. However, as will be demonstrated in Section 3, dE/dx- and displacement-disablements of silicon devices may result from irradiations that are within only one order of magnitude of each other in duration. To lay the groundwork for comparing the two types of disablements in Section 3, we here first relate the displacement damage capability of protons to that of 1-MeV neutrons, since the fluence of such neutrons that would disable various semiconductors via the displacement mechanism is known (e.g., see Ref. 2).

As customary in the radiation effects field, we assume that the degradation of a semiconductor's performance due to displacements is a function of the displacement number-density, independent of the type of radiation that causes the displacements. The induced displacement density is taken to be proportional to the density of primary knock-on atom (PKA) displacements times an average "displacement-effective" PKA recoil energy, $\bar{\omega}$, which is a function of the bombarding particle's energy, E. As fully explained in the Appendix, the total displacement density (PKAs plus all generations of secondary displacements) at depth x of our thick silicon target is proportional to

$$\int_0^\infty (\nu \cdot \bar{\omega}) \cdot \phi(x,E)\, dE.$$

Above, $\Phi(x,E)dE$ represents the fluence of protons at depth x with energies in dE about E, and σ represents the displacement cross section for these protons. Like $\bar{\omega}$, σ is a function of E. The $\Phi(x,E)$ function used in this study is defined by Equation (8) of Reference 4 and the $\sigma \cdot \bar{\omega}$ function is represented by Curve B of Figure 6 of the Appendix.

The curve on the right of Figure 2 represents that portion of the complete $\sigma \cdot \bar{\omega}$ function (the above-cited Curve B) which significantly affects our displacement estimates. If straggling did not occur, all protons would travel to a common depth where all would stop. Also, all would have the same energy at any depth along the way to the common stopping depth. That is, the displacement density at any depth x would simply be proportional to $\sigma(E) \cdot \bar{\omega}(E)$, where E is the common energy that all protons would have at this depth. Since the $\sigma \cdot \bar{\omega}$ function increases by a few orders of magnitude as proton energy is reduced by dE/dx mechanisms, the near-end-of-range displacement density would be some hundredfold larger than the density at the target face, <u>if</u> straggling did not occur.

To help understand the nature of the displacement density distribution to be expected when straggling is taken into account, we have prepared the family of curves shown on the left of Figure 2. There, the solid-line curves give the average proton energy as a function of depth in the silicon target, this average being estimated by use of Equation (10) of Reference 4. The dashed curves, obtained by use of Equation (9) of Reference 4, indicate the percent of the incident protons that remain unstopped at each depth. For the displacement density to be high at a given depth, we would expect two conditions would have to exist at that depth. First, to induce

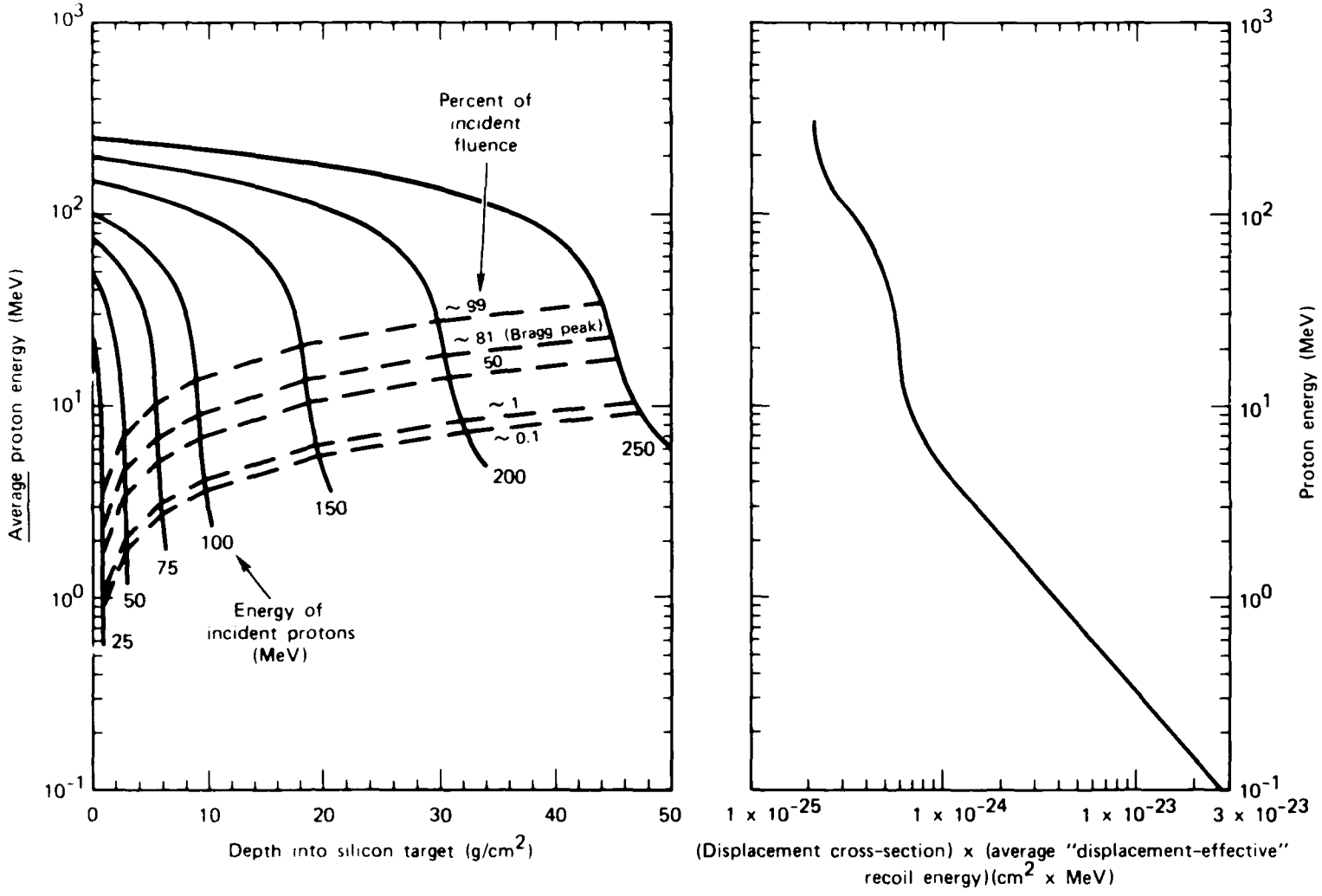

Figure 2. Average energy of unstopped protons (left) and displacement cross-section times average "displacement-effective" recoil energy (right).

a significant number of displacements, the fluence of protons should be a reasonable percentage of the incident fluence. Second, the average energy of the protons should be low so that the quantity $\sigma \cdot \bar{\omega}$, to which the displacement density is proportional, would be high.

Figure 2 permits us to predict the general shape of the displacement-density profile to be expected when a beam of protons of a particular incident energy bombards a thick silicon target. Starting at the target face and moving into the target material, we note that this density should increase initially since the fluence remains essentially constant and the average proton energy drops (i.e., $\sigma \cdot \bar{\omega}$ increases) significantly. As we move to depths near and beyond the Bragg peak, the surviving fluence falls off so fast as to overwhelm the increase in $\sigma \cdot \bar{\omega}$ that results from the lessening of the average proton energy. Hence, we should expect that the displacement density would go to a maximum and then plunge steeply to insignificant levels at points slightly beyond the Bragg peak neighborhood. The lower the incident proton energy, the higher the expected peak of the displacement density, since lower average energies will be realized by a significant fraction of the protons in this neighborhood. However, the penetrability of the lower energy beams is, of course, very low.

In Figure 3, we show a family of curves that have profiles similar to the displacement-density profiles. The ordinate of any point on a curve represents a dimensionless ratio. This ratio equals the value of the integral defined in the second paragraph of this section divided by $\Phi_O \cdot \sigma_N \cdot \bar{\omega}_N$. Here, Φ_O is a fluence equal to the total proton fluence at the face

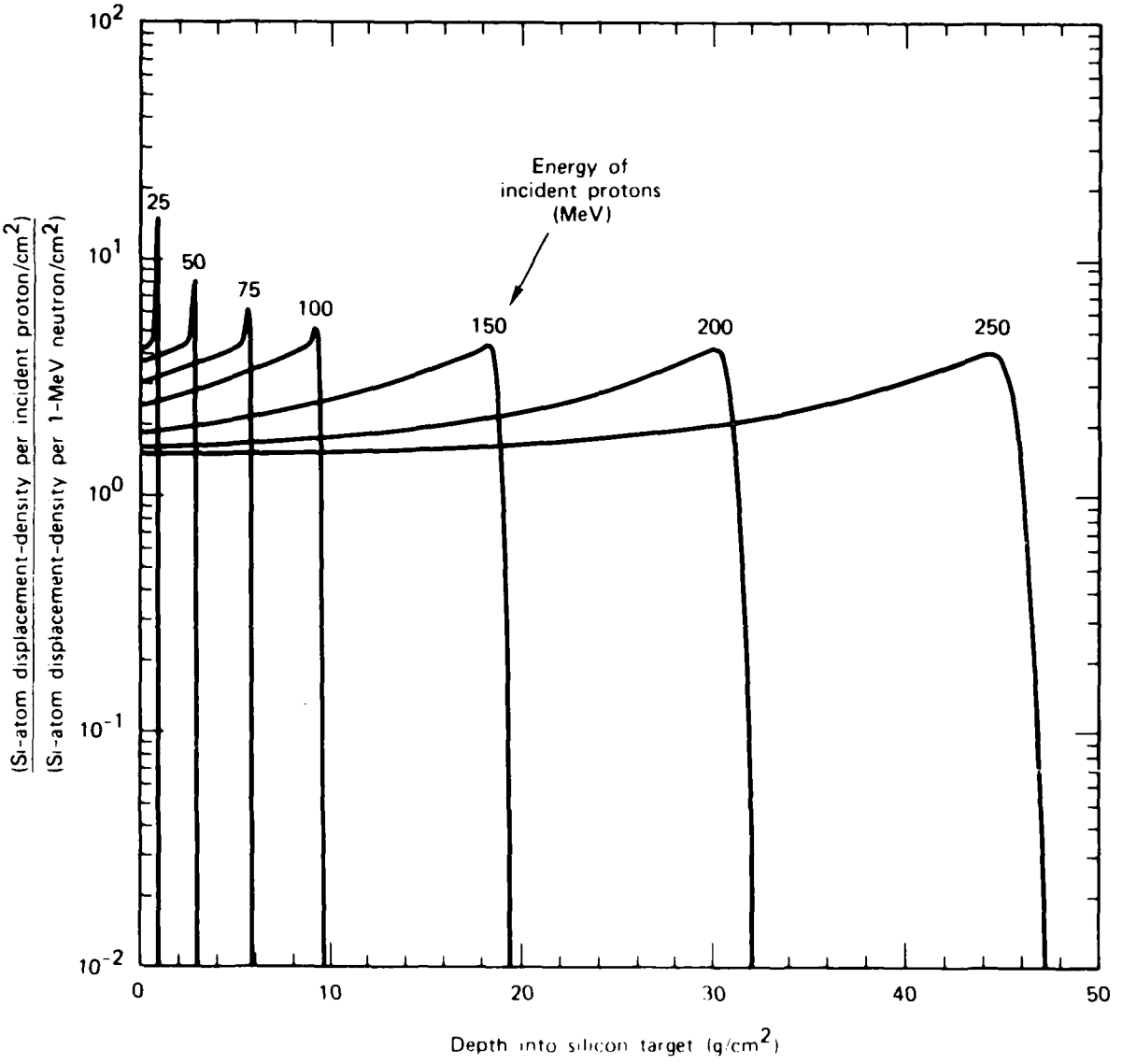

Figure 3. Comparison of estimated proton-induced and 1-MeV-neutron-induced silicon-atom displacement-densities.

of our thick silicon target; $\sigma_N (\cong 3.3 \times 10^{-24}\ cm^2)$ represents the scattering cross section of silicon assumed for 1-MeV neutrons (Ref. 14); and $\bar{\omega}_N (= 0.6 \times [2 \times 28/29^2] \times 1 = 0.040$ MeV) is taken as the average recoil energy of a silicon nucleus when bombarded by 1-MeV neutrons. The 0.6 factor in the $\bar{\omega}_N$ computation is that cited in Reference 11 to account for the forward scattering of MeV neutrons in the center-of-mass system. These assumed data give $\sigma_N \cdot \bar{\omega}_N = 1.33 \times 10^{-25}$ MeV·cm^2 for the 1-MeV neutron displacement kerma.

As noted in Figure 3, the ordinate compares the silicon-atom displacement density at a given depth per proton/cm^2 entering the target at its face with the density that would result if the silicon at that same depth were exposed to a 1-MeV neutron fluence of 1 neutron/cm^2. The essential point here is that we compare displacement densities that arise from a uniform proton bombardment of a surface (that of the target face) with a uniform neutron irradiation of a volume (that of the thick silicon target), the incoming proton fluence and the neutron fluence being equal. This particular ratio readily lends itself to the accomplishment of our primary objective--a comparison of a proton beam's capability to disable a silicon semiconductor via excessive ionization/excitation with its capability to disable via excessive displacements.

SECTION 3

IONIZATION VERSUS DISPLACEMENT DISABLEMENT OF BIPOLAR DEVICES

According to the state-of-the-art hardness levels cited in Reference 2, typical bipolar technology silicon devices can survive an average total ionizing dose of 1 Mrad and the effects of displacements induced by exposure to an average fluence of 10^{14} 1-MeV neutrons/cm^2. For reference purposes, let us adopt the 1-Mrad figure as the average total dose required for the permanent disablement of a silicon device. Also, for reference purposes, let us assume that the displacement-density induced by exposing a device to an average fluence of 10^{14} 1-MeV neutrons/cm^2 is sufficient for permanent disablement. For these selected reference criteria, we now compare the times required for a given proton beam to kill a device via total dose with that required for a displacement kill.

In Figure 4, we show estimates of the two kill times for irradiations by a beam flux of 10^{13} protons/$cm^2 \cdot s$. The family of solid curves gives the estimated total-dose kill time for an assembly of small silicon devices, the totality of which is assumed to make up the equivalent of a thick silicon target. The dashed curves give the estimated times for displacement kills. The kill time for a device that is located where the fluence is attenuated to 0.1% of its incident value is about two orders of magnitude larger than that for a device situated at any depth less than the mean proton range. This is a reason for our terminating the curves at the 0.1% fluence points.

As seen in Figure 4, which is based on the reference kill criteria, disablement via total dose would occur prior to

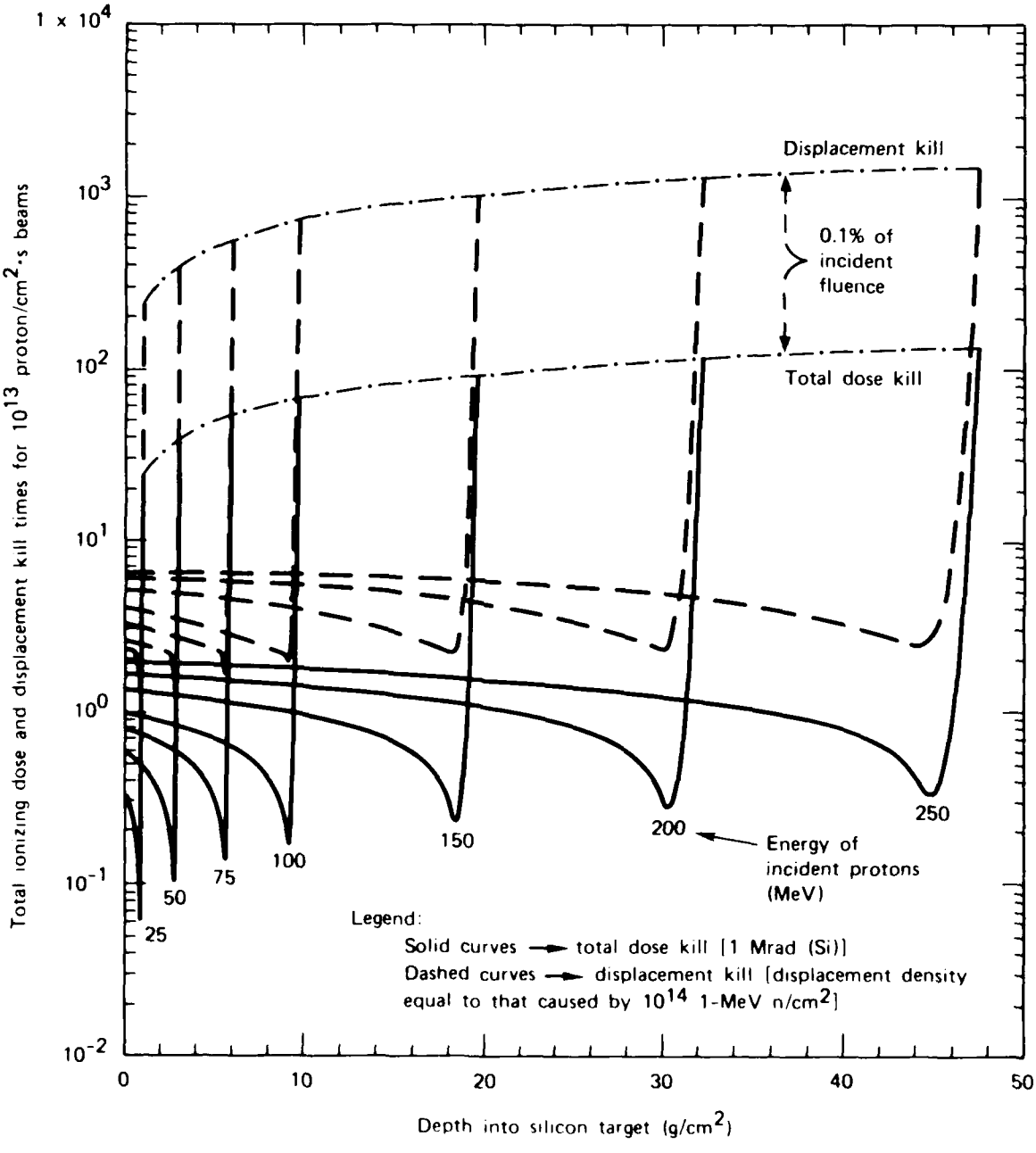

Figure 4. Total dose and displacement damage kill times for 10^{13} P/cm^2.s beams.

disablement via excessive displacements. In Figure 5, we show the ratio of the dose-kill time to the displacement-kill time for the reference criteria. We conclude that kills via total dose should occur in ~1/10 to ~1/5 of the times required for displacement kills for devices hardened to the levels cited on Figures 4 and 5.

It may be noted that the ratio of ionization-to-displacement kill times, of course, scales directly with the ionization dose kill criterion and inversely as the displacement kill criterion. For example, a device which fails (via displacements) upon exposure to only 10^{13} 1-MeV neutrons/cm^2 or to our reference 1-Mrad ionization dose, would experience--essentially simultaneously--a killing level of displacement and also a killing level of ionization. If this same displacement-sensitive device was so "total-dose-robust" as to require 10 Mrads for ionization disablement, it would first be killed by the displacement mechanism and, considerably later, be killed again by excessive ionization.

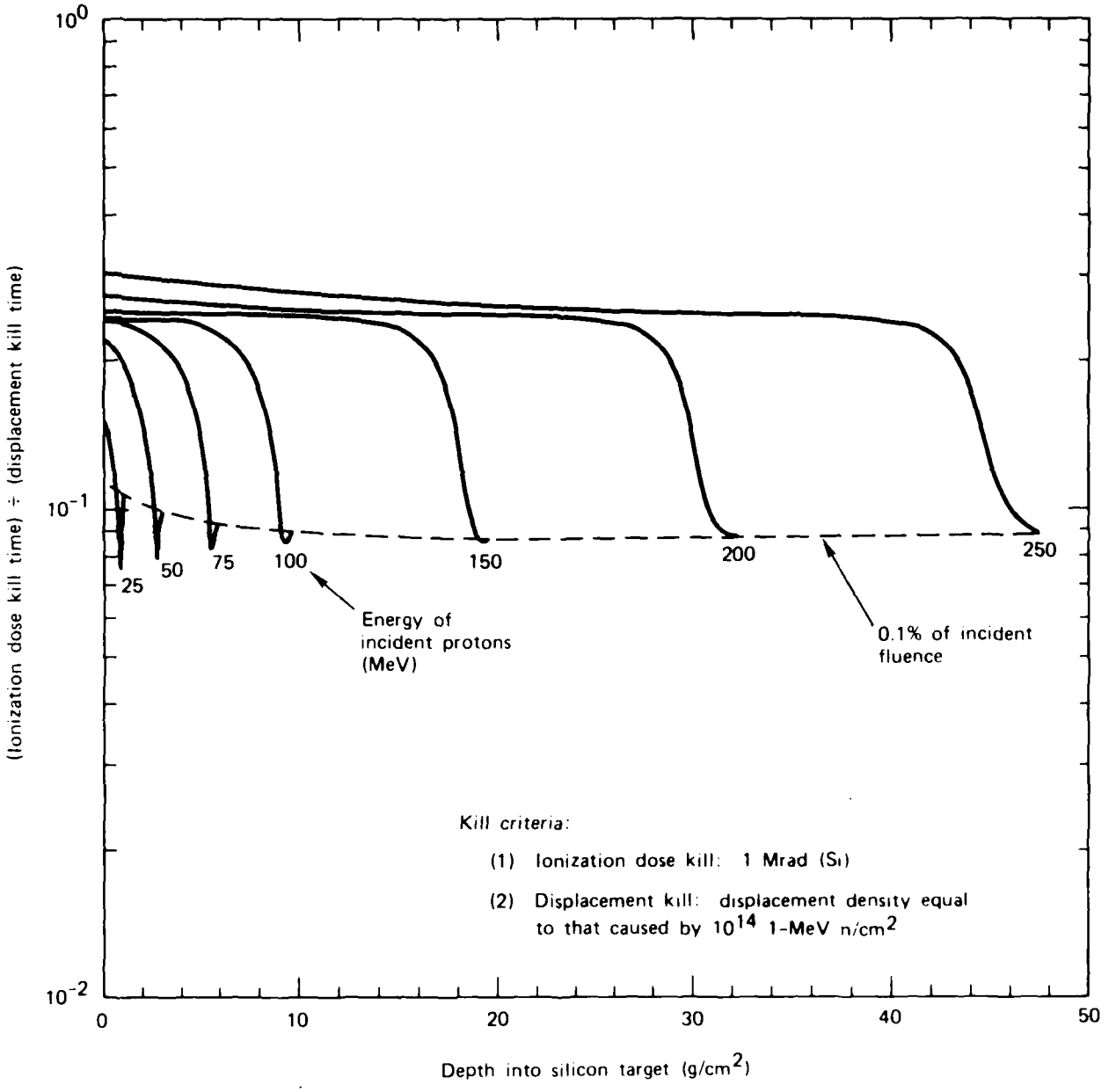

Figure 5. Ratio of total ionization dose kill time to displacement kill time.

SECTION 4

CONCLUDING REMARKS

At the beginning of this study, we planned to examine the effects of silicon bombardment by each of the three hydrogen isotopes (i.e., by deuterons and tritons as well as by protons). Although the two heavier isotopes cannot penetrate target material as deeply as can protons of equal energy, they are more damaging. For example, at points reachable by the heavier isotopes, both the dE/dx energy deposition density and the displacement number-density will be higher than the corresponding insults induced by protons. It was simple enough to estimate the dE/dx energy deposition caused by each of the three isotopes by use of the Reference 4 fluence model. The total dose profiles for the trio of projectiles have, in fact, been computed on the basis of that model (Ref. 5). However, we have thus far only estimated the magnitudes of peak displacement densities to be expected when a thick silicon target is bombarded by each of the three isotopes (Ref. 5).

Now, Rutherford scattering is the likely dominant displacement mechanism as a hydrogen isotope nears the end of its trip into a thick silicon target. And, since the maximum displacement density occurs near the journey's end, it was possible to estimate the peak displacement-density for each type of projectile particle by use of the Rutherford model. However, to develop the complete displacement profiles, one needs a reasonable representation of the displacement damage coefficient (i.e., the $\sigma \cdot \bar{\omega}$ function) at high projectile energies where the simple Rutherford model is not applicable. In the case of proton projectiles, the shape of the $\sigma \cdot \bar{\omega}$ function over much--but not all--of the high-energy range had been established by the Bell Laboratory proton experiments (Ref. 6). As explained in the Appendix, those experiments--

together with the material presented in References 7, 8 and 9--made it possible for us to construct a $\sigma \cdot \bar{\omega}$ function over the full high-energy range needed for the proton-induced displacement estimates presented here.

At this writing, we do not have experimental $\sigma \cdot \bar{\omega}$ data for the bombardment of silicon by high-energy deuterons or tritons. Experiments, similar to those conducted by Bell Laboratory workers using protons within a limited energy range, should be performed using each of the three hydrogen isotopes over an energy range reaching to ~300 MeV. Such thin-target experiments* would establish the shapes of the $\sigma \cdot \bar{\omega}$ functions for each of the three projectile types in the complex high-energy regime, a regime that--at its lower end--overlaps (and is normalizable to) the $\sigma \cdot \bar{\omega}$ functions in the Rutherford scattering regime.

Pending the performance of the above types of experiments, we plan to construct $\sigma \cdot \bar{\omega}$ functions for the two multiple-nucleon hydrogen isotopes (deuterons and tritons) by a procedure similar to that used for the simple single-nucleon projectile, the proton. That procedure (see Appendix) will have to be modified to account for the nearly-simultaneous bombardment of silicon nuclei by two or three nucleons, those initially assembled in the rather weakly bound configuration that represents a deuteron or a triton. Armstrong and Colborn have described a model by which such high-energy bombardments may be treated as a sequence of single nucleon interactions (Ref. 10). We plan to examine that model as a possible means to construct the $\sigma \cdot \bar{\omega}$ functions for deuteron and triton beams.

*In addition to thin-target exposures to highly monoenergetic projectiles, thick-target experiments would, of course, also be desirable since these could reveal the smearing effects of straggling by direct observation.

With these functions in hand, we would be able to repeat for the heavier hydrogen isotopes that which we have reported here for proton beams. This would complete the tasks that we had in mind at the beginning--to estimate the relative vulnerabilities of silicon semiconductor to disablements via excessive ionization and via displacements as such would be induced by hydrogen isotope bombardment.

SECTION 5

LIST OF REFERENCES

1. Van Lint, V., et al, Mechanisms of Radiation Effects in Electronic Materials, Vol. 1, p. 270, John Wiley and Sons, 1980.

2. Long, D. M., "State-of-the-Art Review: Hardness of MOS and Bipolar Integrated Circuits," IEEE Transactions on Nuclear Science, Vol. NS-27, No. 6, p. 1674, December 1980.

3. Mather, R., and Segre, E., "Range Energy Relation for 340-MeV Protons," Physical Review, Vol. 84, No. 2, p. 191, 15 October 1951.

4. Safonov, G., A Model for Estimating Particle Beam Effects in the Bragg Peak Neighborhood, RDA-TR-130010-003, R & D Associates, Marina del Rey, CA, October 1984.

5. Safonov, G., Status of Some Recent In-House Work on the DNA DEW Subtask 10.4: Neutral Particle Beam Effects--Specifically, NPB Effects on Electronics, An Internal R & D Associates Memorandum, 7 December 1984.

6. Rosenzweig, W., et al., "Energy Dependence of Proton Irradiation Damage in Silicon," Journal of Applied Physics, Vol. 35, No. 9, p. 2707, September 1964.

7. More, R. M., et al, "Primary Recoil Spectra and Subcascade Effects in Ion Bombardment Experiments," Radiation Effects, Vol. 60, p. 27, Gordon and Breach Science Publishers, Inc., Great Britain, 1982.

8. Wood, S., et al., "Simulation of Radiation Damage in Solids," IEEE Transactions on Nuclear Science, Vol. NS-28, No. 6, p. 4107, December 1981.

9. Konshin, V. A., and Matusevich, E. S., "Characteristics of the Interaction of High-Energy Nucleons with Nuclei," Atomic Review, Vol. 6, No. 4, p. 3, International Atomic Agency, 1968.

10. Armstrong, T.W. and Colborn, B. L., "A Thick-Target Radiation Transport Computer Code for Low-Mass Heavy Ion Beams," Nuclear Instruments and Methods, Vol. 169, p. 161, 1980.

11. Dienes, G. J., and Vineyard, G. H., Radiation Effects in Solids, Volume II, Interscience Publishers, Inc., New York, NY, 1957.

12. Baicker, J. A., et al., "Proton Induced Lattice Displacements in Silicon," Applied Physics Letters, Vol. 2, No. 5, p. 104, 1 March 1963.

13. Thatcher, R. K., editor, Transient-Radiation Effects on Electronics Handbook, Edition No. 2, Revision No. 1, DASA 1420, Defense Atomic Support Agency, Washington, DC, August 1967.

14. Hughes, D. J., and Harvey, J. A., Neutron Cross Sections, BNL 325, Brookhaven National Laboratory, July 1, 1955.

APPENDIX:

ASSUMED REPRESENTATION OF THE DISPLACEMENT DAMAGE FUNCTION

Provided that a proton-bombarded silicon atom's recoil energy is not too high but high enough to cause its displacement from its normal position in the crystalline lattice, the total number of displacements (primary plus all secondaries) has often been taken to be proportional to the recoil energy of the primary knock-on atom (e.g., see p. 27 of Ref. 11; p. 104 of Ref. 12; and, p. E-3 of Ref. 13). However, as has been noted more recently in References 7 and 8, there is considerable experimental evidence that the energy in a displacement cascade does not increase indefinitely with increasing primary recoil energy. Thus, for the recoil energies of primary knock-on atoms (PKAs) that result from high-energy proton collisions with silicon nuclei (i.e., where proton energy $\gtrsim$ coulomb barrier energy), the total number of displacements will be proportional to an average "displacement-effective" recoil energy, which is less than the average PKA energy.

The fluence of protons with energies in dE about E at depth x in a silicon target is denoted by $\phi(x,E)dE$. This incremental portion of the total fluence at x will cause a displacement density proportional to $\sigma(E)\cdot\bar{\nu}(E)\cdot\phi(x,E)dE$. Here, $\sigma(E)$ is the displacement cross section for protons of energy E, and $\bar{\nu}(E)$ is the average of the "displacement-effective" recoil energies for such protons. We refer to the product $\sigma\bar{\nu}$ as a displacement damage function since the total displacement density per proton is taken to be proportional to this function of proton energy. As noted above, since $\bar{\nu} < \bar{T}_{PKA}$ (the average PKA recoil energy), $\sigma\bar{\nu} < \sigma\bar{T}_{PKA}$. Figure 6 displays our assumed representations of $\sigma\bar{T}_{PKA}$ (Curve A) and $\sigma\bar{\nu}$ (Curve B).

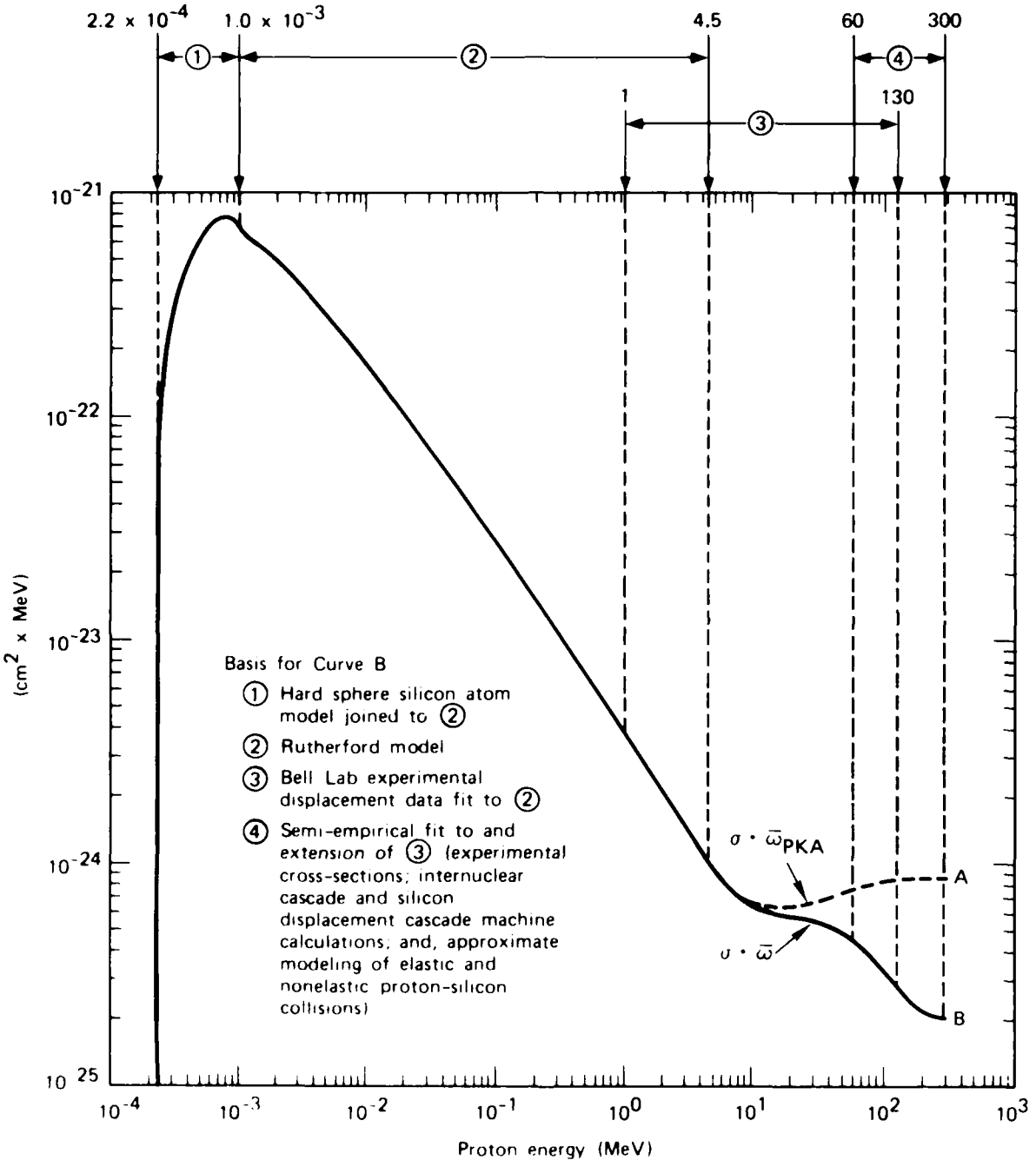

Figure 6. Assumed representations of displacement cross-section times average recoil energy of primary knock-on atoms (Curve A) and times average "displacement-effective" recoil energy (Curve B) for proton bombardment of silicon crystal.

As indicated on the figure, our $\sigma \cdot \bar{\omega}$ function was constructed to conform with available experimental data plus certain computed information. It is convenient to describe the construction in terms of four bases, denoted by ①, ②, ③, and ④ on the figure. Basis ③, which refers to the 1964 experiments by Bell Laboratory staff (Ref. 6), is central to the overall construction of Curve B. These workers irradiated silicon solar cells by protons in the 1- to 130-MeV range and determined the dependence of the displacement damage coefficient on proton energy within this range. They observed that--at the beginning of the range investigated--the coefficient decreased with increasing proton energy as predicted by the Rutherford scattering model. Accordingly, we fit the experimental Bell curve to the $\sigma \cdot \bar{\omega}_{PKA}$ curve computed by use of the Rutherford model (see overlapping of segments ② and ③ in Figure 6).

According to the prescription of Equation 2-8 of Reference 11, we assumed the Rutherford model to apply for proton energies down to ~1 KeV and the hard sphere silicon atom model to apply for energies between 1 KeV and ~220 eV, the range of curve segment ①. The 220-eV figure represents the lowest energy that a proton can have and still displace a silicon atom (30 eV has been assumed for the minimum silicon recoil energy needed for a displacement to occur). The collision cross section of the silicon atom in the segment-① energy interval is assumed to vary linearly with proton energy. For an atom at rest, we assume a radius equal to the Bohr radius of the atom's outer electrons. The cross section for 1-KeV protons is adjusted to give a continuous $\sigma \cdot \omega$ function where segments ① and ② join.

As seen in Figure 2 of the text, the number of protons that are slowed to an average energy of less than 100 KeV is

estimated to be negligible by use of the $\varphi(x,E)$ model used in this study. Hence, our estimates of displacement densities cannot be sensitive to the assumed form of the $\sigma\cdot\bar{\omega}$ function in and near the segment-① regime of Figure 6.

Unfortunately, the 130-MeV upper limit of the proton-energies used in the Bell Laboratory experiments falls short of the nominal 250-MeV maximum of interest to us here. To extend Curve B to cover the desired high-energy range, we generated segment-④, which runs from 60 MeV to 300 MeV and reasonably fits the Bell data in the 60- to 130-MeV range. For proton energies in the segment-④ range, $\sigma\cdot\bar{\omega}_{PKA}$ has an elastic collision component, $\sigma_e\cdot(\bar{\omega}_e)_{PKA}$, and nonelastic collison component, $\sigma_n\cdot(\bar{\omega}_n)_{PKA}$.

To estimate the elastic component, we assert all protons are scattered by a small angle equal to the proton's de Broglie wavelength divided by a certain diameter. The diameter is that of a circle whose area equals σ_e, the elastic scattering cross section for proton-silicon collisions. This assertion yields

$$\sigma_e\cdot(\bar{\omega}_e)_{PKA} = \pi\frac{h^2}{8M}\ , \qquad (2)$$

where M is the mass of the silicon nucleus and h is Plank's constant. The above gives 0.[illegible] x 10^{-24} $cm^2\cdot MeV$ for the elastic component.

The nonelastic component is estimated by assuming that the proton collides elastically with one of the nucleons in the silicon nucleus and also that the following conditions apply. Whichever of the two colliding nucleons emerges from the encounter with the greatest energy is assumed to move on a

straight line and--without further encounters--to leave the nucleus. The nucleon emerging from the collision with the lesser energy is assumed to be stopped within the nucleus. The momentum of this trapped nucleon goes over to the nucleus formed by the entrapment. The energy of this nucleon goes to $(\bar{\omega}_n)_{PKA}$; to excitation energy, E*, of the compound system; and, to rotational energy, which we neglect in estimating the nonelastic component of $\sigma \cdot \bar{\omega}_{PKA}$. Where these conditions apply, one finds

$$\sigma_n \cdot (\bar{\omega}_n)_{PKA} = \sigma_n \cdot \frac{m}{M-m} \cdot \bar{E}^* \ , \qquad (3)$$

where m is the proton mass and $\bar{E}^*$ is the average value of E*. We use the 1968 Soviet Monte Carlo computations for $\bar{E}^*$ [see p. 46 of Ref. 9]. And, for lack of better information at this time, we assume the nonelastic cross section, σ_n, for proton bombardment of silicon-28 equals that for proton bombardment of aluminum-27. Experimental values of σ_n for aluminum are taken from page 9 of the same Soviet paper just cited.

The sum of the two components of $\sigma \cdot \bar{\omega}_{PKA}$ thus estimated is represented by that portion of Curve A in Figure 6 that lies in the proton energy interval of 60 to 300 MeV. To estimate the corresponding portion of the $\sigma \cdot \bar{\omega}$ function (i.e., Curve B), we looked to References 7 and 8 for guidance.

As previously implied, the authors of those two papers taught us that--for high-energy recoils--the "displacement-effective" average recoil energy, $\bar{\omega}$, does not remain proportional to the average of the actual PKA recoil energy, $\bar{\omega}_{PKA}$. Rather, the

ratio $\bar{\omega}/\bar{\omega}_{PKA}$ decreases with increasing $\bar{\omega}_{PKA}$. For protons with energies between 60 and 130 MeV, we could fit the Bell Laboratory experimental findings by assuming that $\bar{\omega} = \bar{\omega}_{PKA}$ if $\bar{\omega}_{PKA} < 0.35$ MeV and that $\bar{\omega} = 0.35$ MeV if $\bar{\omega}_{PKA} > 0.35$ MeV. This, together with the assumption that silicon nonelastic--as well as elastic--cross sections equaled those for aluminum (as presented on p. 9 of Ref. 9), permitted us to extend Curve B from 130-MeV to 300-MeV proton energies in the manner shown in Figure 6.

With the 0.35-MeV limit on $\bar{\omega}$, we have the following prescriptions for the two components of $\sigma \cdot \bar{\omega}$ in the segment-④ energy interval.

$$\sigma_e \cdot \bar{\omega}_e = 0.23 \times 10^{-24} \text{ cm}^2 \cdot \text{MeV}; \quad 60 < E < 90 \text{ MeV}, \qquad (4a)$$

$$\sigma_e \cdot \bar{\omega}_e = 0.35 \times \sigma_e \text{ cm}^2 \cdot \text{MeV}; \quad 90 < E < 300 \text{ MeV}, \qquad (4b)$$

and

$$\sigma_n \cdot \bar{\omega}_n = 0.35 \times \sigma_n \text{ cm}^2 \cdot \text{MeV}; \quad 60 < E < 300 \text{ MeV}. \qquad (4c)$$

Above, E represents proton energy and the σ's are implied to be in units of cm^2. The initial fall-off and then flattening of Curve B for E > 60 MeV result from the similar behaviors of the σ's as functions of E (see p. 9 of Ref. 9).

DISTRIBUTION LIST

DEPARTMENT OF DEFENSE

ASST TO THE SEC OF DEFENSE ATOMIC ENERGY
ATTN: EXEC ASST DEF RSCH & ENGRG
ATTN: STRAT & SPACE SYS(OS)
ATTN: STRAT & THEATER NUC FOR F VAJDA

DEFENSE ADVANCED RSCH PROJ AGENCY
ATTN: R REYNOLDS
ATTN: S ROOSILD

DEFENSE COMMUNICATIONS ENGINEER CENTER
ATTN: CODE R720 C STANSBERRY

DEFENSE ELECTRONIC SUPPLY CENTER
ATTN: DEFC EAA

DEFENSE INTELLIGENCE AGENCY
ATTN: DT 1B
ATTN: RTS 2B

DEFENSE LOGISTICS AGENCY
ATTN: DLA QEL W T HUDDLESON
ATTN: DLA SEE F HARRIS

DEFENSE NUCLEAR AGENCY
2 CYS ATTN: RAEV (TREE)
2 CYS ATTN: STTI CA

DEFENSE TECHNICAL INFORMATION CENTER
2 CYS ATTN: DD

DNA PACOM LIAISON OFFICE
ATTN: J BARTLETT

FIELD COMMAND DEFENSE NUCLEAR AGENCY
ATTN: FCPE R ROBINSON
ATTN: FCTT
ATTN: FCTT W SUMMA
ATTN: FCTXE

FIELD COMMAND DNA DET 2
LAWRENCE LIVERMORE NATIONAL LAB
ATTN: FC 2

JOINT CHIEFS OF STAFF
ATTN: C3S EVALUATION OFFICE (HDOO)

JOINT DATA SYSTEMS SUPPORT CTR
ATTN: C JEAN R MASON
ATTN: C JEAN

JOINT STRAT TGT PLANNING STAFF
ATTN: JPTP ATTN: DNA REP
ATTN: JPTS
ATTN: JPPFD
ATTN: JPTM
ATTN: JPTC

NATIONAL COMMUNICATIONS SYSTEM
ATTN: NCS TS
ATTN: NCS TS D BODSON

DEPARTMENT OF THE ARMY

HARRY DIAMOND LABORATORIES
ATTN: SCHLD:NW:P
ATTN: SLCHD:NW:EC
ATTN: SLCHD:NW:EC J MILETTA
ATTN: SLCHD:NW:R
ATTN: SLCHD:NW:R F MCLEAN 22300
ATTN: SLCHD:NW:RA
ATTN: SLCHD:NW:RC
ATTN: SLCHD:NW:RH

NUCLEAR EFFECTS DIVISION
ATTN: R WILLIAMS

U S ARMY ARMOR & ENGINEER BOARD
ATTN: ATZK AE AR J DENNIS

U S ARMY BALLISTIC RESEARCH LAB
ATTN: SLCBR VL D RIGOTTI

U S ARMY COMMUNICATIONS R&D COMMAND
ATTN: DRSEL NL RO R BROWN

U S ARMY ELECTRONIC TECH DEV LAB
ATTN: SLCET SI R ZETO

U S ARMY ENGINEER DIV HUNTSVILLE
ATTN: HNDED ED J HARPER

U S ARMY MATERIAL TECHNOLOGY LABORATORY
ATTN: DRXMR B J HOFMANN
ATTN: DRXMR HH J DIGNAM

U S ARMY NUCLEAR & CHEMICAL AGENCY
ATTN: LIBRARY

U S ARMY RESEARCH OFFICE
ATTN: R GRIFFITH

U S ARMY STRATEGIC DEFENSE CMD
ATTN: BMDSC AV T HARPER
ATTN: BMDSC HW R DEKALB
ATTN: DASD H SAV
ATTN: DASD H SAV R C WEBB

U S ARMY STRATEGIC DEFENSE COMMAND
ATTN: ATC O E HOKE
ATTN: ATC T

U S ARMY TEST AND EVALUATION COMD
ATTN: AMSTE

U S ARMY TRADOC SYS ANALYSIS ACTVY
ATTN: ATAA TEC COMMANDER

DEPARTMENT OF THE ARMY (CONTINUED)

US ARMY MISSILE COMMAND
ATTN: AMSMI-LC-FS G THURLOW
ATTN: HAWK PROJ OFCR AMCPM-HA-SE-MS
3 CYS ATTN: REDSTONE SCIENTIFIC INFO CTR

US ARMY WHITE SANDS MISSILE RANGE
ATTN: STEWS-DE-DT R HAYS
ATTN: STEWS-TE-AN A DE LA PAZ
ATTN: STEWS-TE-AN J MEASON
ATTN: STEWS-TE-AN R DUTCHOVER
ATTN: STEWS-TE-N K CUMMINGS
ATTN: STEWS-TE-N T ARELLANES
ATTN: STEWS-TE-NT M SQUIRES

USAG
ATTN: TECH REF DIV

XM-1 TANK SYSTEM
ATTN: DRCPM-GCM-SW

DEPARTMENT OF THE NAVY

NAVAL AIR SYSTEMS COMMAND
ATTN: AIR-350F
ATTN: AIR-54042
ATTN: AIR-931A

NAVAL AVIONICS CENTER
ATTN: CODE B455 D REPASS

NAVAL ELECTRONICS ENGRG ACTVY, PACIFIC
ATTN: CODE 250 D OBRYHIM

NAVAL INTELLIGENCE SUPPORT CTR
ATTN: NISC LIBRARY

NAVAL OCEAN SYSTEMS CENTER
ATTN: CODE 9642 TECH LIB

NAVAL POSTGRADUATE SCHOOL
ATTN: CODE 1424 LIBRARY

NAVAL RESEARCH LABORATORY
ATTN: CODE 4040 J BORIS
ATTN: CODE 4154 J H ADAMS
ATTN: CODE 4600 D NAGEL
ATTN: CODE 4610 J RITTER
ATTN: CODE 4611 E PETERSON
ATTN: CODE 4612 D WALKER
ATTN: CODE 4613 A B CAMPBELL
ATTN: CODE 4614 L A GUST
ATTN: CODE 4652 G MUELLER
ATTN: CODE 4653 A NAMENSON
ATTN: CODE 4673 A PENTOSON
ATTN: CODE 4682 C FROZIER
ATTN: CODE 4682 S BROWN
ATTN: CODE 5813 N SAKS
ATTN: CODE 5813 W JENKINS
ATTN: CODE 5814 D MCCARTHY
ATTN: CODE 5814 M PECKERAR
ATTN: CODE 5816 E D RICHMOND
ATTN: CODE 5816 R HEVEY
ATTN: CODE 5816 R LAMBERT
ATTN: CODE 6810 J KILLIANY
ATTN: CODE 6816 H HUGHES

NAVAL SEA SYSTEMS COMMAND
ATTN: CODE 08K NEWHOUSE

NAVAL SURFACE WEAPONS CENTER
ATTN: CODE F31 F WARNOCK
ATTN: CODE H23 R SMITH

NAVAL SURFACE WEAPONS CENTER
ATTN: CODE H 21

NAVAL UNDERWATER SYS CENTER
ATTN: 8092

NAVAL WEAPONS CENTER
ATTN: CODE 343 FKA6A2 TECH SVCS

NAVAL WEAPONS EVALUATION FACILITY
ATTN: CLASSIFIED LIBRARY

NAVAL WEAPONS SUPPORT CENTER
ATTN: CODE 605 J RAMSEY
ATTN: CODE 6054 D PLATTETER
ATTN: CODE 6054 T ELLIS

OFC OF THE DEP ASST SEC OF THE NAVY
ATTN: L J ABELLA

OFC OF THE DEPUTY CHIEF OF NAVAL OPS
ATTN: NOP 985F

OFFICE OF NAVAL RESEARCH
ATTN: CODE 1114

OPERATIONAL TEST & EVALUATION FORCE
ATTN: CODE 80

SPACE & NAVAL WARFARE SYSTEMS CMD
ATTN: CODE 5045 11 C SUMAN
ATTN: CODE 50451
ATTN: NAVELEX 51024 C WATKINS
ATTN: PME 117 21

STRATEGIC SYSTEMS PROGRAM OFFICE (PM-1)
ATTN: NSP-2301
ATTN: NSP-2701
ATTN: NSP-27331
ATTN: NSP-27334

DEPARTMENT OF THE AIR FORCE

AERONAUTICAL SYSTEMS DIVISION
ATTN: ASD/ENES P MARTH
ATTN: ASD/ENSS

AIR FORCE CTR FOR STUDIES & ANALYSIS
2 CYS ATTN: AFCSA/SAMI R GRIFFIN

AIR FORCE GEOPHYSICS LABORATORY
ATTN: SULL

AIR FORCE INSTITUTE OF TECHNOLOGY/EN
ATTN: AFIT/ENP C BRIDGMAN
ATTN: LIBRARY/AFIT/LDEE

AIR FORCE SYSTEMS COMMAND
ATTN: DLCAM
ATTN: DLW

AIR FORCE WEAPONS LABORATORY, AFSC
ATTN: NTAAB C BAUM
ATTN: NTC M SCHNEIDER
ATTN: NTCAS J FERRY
ATTN: NTCAS J MULLIS
ATTN: NTCT MAJ HUNT
ATTN: NTCTR CAPT RIENSTRA
ATTN: NTCTR R MAIER
ATTN: SUL
ATTN: TA B FREDERICKSON

AIR FORCE WRIGHT AERONAUTICAL LAB
ATTN: POOC-2 J WISE

AIR FORCE WRIGHT AERONAUTICAL LAB
ATTN: AFWAL/AADE
ATTN: AFWAL/MLTE

AIR UNIVERSITY LIBRARY
ATTN: AUL-LSE

BALLISTIC MISSILE OFFICE/DAA
ATTN: ENFI
ATTN: ENSE
ATTN: ENSN

ELECTRONIC SYSTEMS DIVISION/IN
ATTN: INDC

FOREIGN TECHNOLOGY DIVISION, AFSC
ATTN: R MAINGER

OFFICE OF SPACE SYSTEMS
ATTN: DIRECTOR

OGDEN AIR LOGISTICS COMMAND
ATTN: OO-ALC/MMEDD/HARD CONTROL
ATTN: OO-ALC/MMGR/DOC CONTROL

OKLAHOMA CITY AIR LOGISTICS CTR
ATTN: DMM/R WALLIS

ROME AIR DEVELOPMENT CENTER, AFSC
ATTN: RBR J BRAUER

ROME AIR DEVELOPMENT CENTER, AFSC
ATTN: ESR J SCHOTT
ATTN: ESR W SHEDD

SPACE DIVISION/AQ
ATTN: ALT

SPACE DIVISION/YA
ATTN: YAS

SPACE DIVISION/YAR
ATTN: YAR CAPT STAPANIAN

SPACE DIVISION/YD
ATTN: YD

SPACE DIVISION/YE
ATTN: YE

SPACE DIVISION/YG
ATTN: YG

SPACE DIVISION/YN
ATTN: YN

STRATEGIC AIR COMMAND/INA
ATTN: INA

STRATEGIC AIR COMMAND/NRI-STINFO
ATTN: NRI/STINFO

STRATEGIC AIR COMMAND/XPFC
ATTN: XPFC

TACTICAL AIR COMMAND/XPJ
ATTN: TAC/XPJ

3416TH TECHNICAL TRAINING SQUADRON (ATC)
ATTN: TTV

DEPARTMENT OF ENERGY

DEPARTMENT OF ENERGY
ATTN: ESHD

UNIVERSITY OF CALIFORNIA
LAWRENCE LIVERMORE NATIONAL LAB
ATTN: L-13 D MEEKER
ATTN: L-156 J YEE
ATTN: L-156 R KALIBJIAN
ATTN: L-53 TECH INFO DEPT LIB
ATTN: L-84 H KRUGER
ATTN: W ORVIS

DEPARTMENT OF ENERGY (CONTINUED)

LOS ALAMOS NATIONAL LABORATORY
ATTN: D LYNN
ATTN: E LEONARD

SANDIA NATIONAL LABORATORIES
ATTN: ORG 2100 B L GREGORY
ATTN: ORG 2126 J E GOVER
ATTN: ORG 2144 P V DRESSENDORFER
ATTN: ORG 2146 T A DELLIN
ATTN: ORG 2150 J A HOOD
ATTN: ORG 2320 J H RENKEN
ATTN: ORG 2321 L D POSEY
ATTN: ORG 5152 J L DUNCAN
ATTN: T F WROBEL

OTHER GOVERNMENT

CENTRAL INTELLIGENCE AGENCY
ATTN: OSWR/NED
ATTN: OSWR/STD/MTB

DEPARTMENT OF TRANSPORTATION
ATTN: ARD-350

NASA
ATTN: CODE 313 V DANCHENKO
ATTN: CODE 600 E STASSINOPOULOS
ATTN: CODE 660 J TRAINOR
ATTN: CODE 695 M ACUNA
ATTN: CODE 724.1 M JHABVALA

NASA
ATTN: M BADDOUR

NASA HEADQUARTERS
ATTN: CODE DP B BERNSTEIN

NATIONAL BUREAU OF STANDARDS
ATTN: C WILSON
ATTN: CODE A327 H SCHAFFT
ATTN: CODE A347 J MAYO-WELLS
ATTN: CODE A353 S CHAPPELL
ATTN: CODE A361 J FRENCH
ATTN: CODE C216 J HUMPHREYS
ATTN: T RUSSELL

DEPARTMENT OF DEFENSE CONTRACTORS

ADVANCED RESEARCH & APPLICATIONS CORP
ATTN: L PALKUTI
ATTN: R ARMISTEAD

AEROJET ELECTRO SYSTEMS CO
ATTN: D TOOMB B 160 D 4343
ATTN: P LATHROP

AEROSPACE CORP
ATTN: C E BARNES
ATTN: D FRESH
ATTN: D SCHMUNK
ATTN: G GILLEY
ATTN: I GARFUNKEL
ATTN: J REINHEIMER
ATTN: J STOLL
ATTN: J WIESNER
ATTN: J B BLAKE
ATTN: K T WILSON
ATTN: M DAUGHERTY
ATTN: N SRAMEK
ATTN: P BUCHMAN
ATTN: R SLAUGHTER
ATTN: W CRANE
ATTN: W KOLASINSKI

ALLIED CORP
ATTN: DOCUMENT CONTROL

ALLIED CORP, BENDIX FLIGHT
ATTN: E MEEDER

AMPEX CORP
ATTN: K WRIGHT
ATTN: P PEYROT

ANALYTIC SERVICES, INC (ANSER)
ATTN: A SHOSTAK
ATTN: J OSULLIVAN
ATTN: P SZYMANSKI

APPLIED SYSTEMS ENGRG DIRECTOR
ATTN: J P RETZLER NUC S/V MANG

AVCO SYSTEMS DIVISION
ATTN: D SHRADER

BDM CORP
ATTN: C M STICKLEY

BDM CORP
ATTN: D WUNSCH

BEERS ASSOCIATES, INC
ATTN: B BEERS

BOEING CO
ATTN: M ANAYA
ATTN: C ROSENBERG
ATTN: A JOHNSTON
ATTN: D EGELKROUT
ATTN: E L SMITH
ATTN: I ARIMURA
ATTN: R CALDWELL
ATTN: W DOHERTY
ATTN: H WICKLEIN

DEPT OF DEFENSE CONTRACTORS (CONTINUED)

BOEING CO (CONTINUED)
ATTN O MULKEY
ATTN C DIXON

CALIFORNIA INSTITUTE OF TECHNOLOGY
ATTN W PRICE

CALSPAN CORP
ATTN R THOMPSON

CHARLES STARK DRAPER LAB, INC
ATTN J BOYLE
ATTN N TIBBETTS
ATTN P GREIFF
ATTN W D CALLENDER

CINCINNATI ELECTRONICS CORP
ATTN L HAMMOND

CLARKSON COLLEGE OF TECHNOLOGY
ATTN P J MCNULTY

COMPUTER SCIENCES CORP
ATTN A SCHIFF

DENVER, UNIVERSITY OF
ATTN SEC OFCR FOR F VENDITTI

DEVELCO, INC
ATTN G HOFFMAN

E SYSTEMS, INC
ATTN K REIS

E SYSTEMS, INC
ATTN DIV LIBRARY

EATON CORP
ATTN R BRYANT

ELECTRONIC INDUSTRIES ASSOCIATION
ATTN J KINN

FMC CORP
ATTN L STATES

FORD AEROSPACE & COMMUNICATIONS CORP
ATTN TECH INFOR SVCS

GARRETT CORP
ATTN S ELLIOTT

GENERAL ELECTRIC CO
ATTN D EDELMAN
ATTN D TASCA
ATTN DOCUMENTS LIB
ATTN H ODONNELL
ATTN: J ANDREWS
ATTN: R BENEDICT
ATTN: R CASEY
ATTN: TECHNICAL LIB

GENERAL ELECTRIC CO
ATTN: B FLAHERTY
ATTN: G BENDER
ATTN: L HAUGE

GENERAL ELECTRIC CO
ATTN: G GATI MD

GENERAL ELECTRIC CO
ATTN: C HEWISON
ATTN: D COLE

GENERAL ELECTRIC CO
ATTN: J MILLER

GENERAL RESEARCH CORP
ATTN: A HUNT

GEORGE WASHINGTON UNIVERSITY
ATTN: A FRIEDMAN

GOODYEAR AEROSPACE CORP
ATTN: SECURITY CONTROL STA

GRUMMAN AEROSPACE CORP
ATTN: J ROGERS

GTE GOVERNMENT SYSTEMS CORPORATION
ATTN: J A WALDRON

HARRIS CORP
ATTN: E YOST
ATTN: W ABARE

HARRIS CORP
ATTN: J W SWONGER

HONEYWELL, INC
ATTN: D HEROLD
ATTN: D LAMB
ATTN: D NIELSEN
ATTN: R BELT
ATTN: R GUMM

HONEYWELL, INC
ATTN J SCHAFER
ATTN MS 725 5

HUGHES AIRCRAFT CO
ATTN R C HENDERSON

HUGHES AIRCRAFT CO
ATTN W SCHENET

DEPT OF DEFENSE CONTRACTORS (CONTINUED)

HUGHES AIRCRAFT CO
ATTN J HALL

HUGHES AIRCRAFT COMPANY
ATTN A NAREVSKY
ATTN E KUBO
ATTN L DARDA

IBM CORP
ATTN H MATHERS

IBM CORP
ATTN J ZIEGLER

IBM CORP
ATTN A EDENFELD
ATTN N HADDAD

IIT RESEARCH INSTITUTE
ATTN A K BUTI
ATTN I MINDEL

ILLINOIS COMPUTER RESEARCH, INC
ATTN E S DAVIDSON

INSTITUTE FOR DEFENSE ANALYSES
ATTN TECH INFO SVCS

IRT CORP
ATTN J AZAREWICZ
ATTN J HARRITY
ATTN J M WILKENFELD
ATTN M ROSE
ATTN MDC
ATTN N RUDIE
ATTN R MERTZ

JAYCOR
ATTN DR M TREADAWAY
ATTN R STAHL
ATTN T FLANAGAN

JAYCOR
ATTN R SULLIVAN

JAYCOR
ATTN C ROGERS
ATTN R POLL

JOHNS HOPKINS UNIVERSITY
ATTN P PARTRIDGE
ATTN R MAURER

JOHNS HOPKINS UNIVERSITY
ATTN G MASSON

KAMAN SCIENCES CORP
ATTN C BAKER
ATTN DIR SCI & TECH DIV
ATTN J ERSKINE
ATTN N BEAUCHAMP
ATTN W RICH

KAMAN SCIENCES CORP
ATTN E CONRAD

KAMAN SCIENCES CORPORATION
ATTN TECH LIB FOR D PIRIO

KAMAN TEMPO
ATTN DASIAC
ATTN R RUTHERFORD
ATTN W MCNAMARA

KAMAN TEMPO
ATTN DASIAC

LITTON SYSTEMS, INC
ATTN E L ZIMMERMAN
ATTN F MOTTER

LOCKHEED MISSILES & SPACE CO, INC
ATTN F JUNGA
ATTN J SMITH
ATTN REPORTS LIB

LOCKHEED MISSILES & SPACE CO, INC
ATTN B KIMURA
ATTN E HESSEE
ATTN J C LEE
ATTN J CAYOT
ATTN L ROSSI
ATTN P BENE
ATTN S TAIMUTY

LTV AEROSPACE & DEFENSE COMPANY
ATTN A.R. TOMME
ATTN LIBRARY
ATTN TECH DATA CTR

MAGNAVOX ADVANCED PRODUCTS & SYS CO
ATTN W HAGEMEIER

MARTIN MARIETTA CORP
ATTN J TANKE
ATTN J WARD
ATTN MP 1601 W BRUCE
ATTN R GAYNOR
ATTN TIC/MP 30

MARTIN MARIETTA CORP
ATTN T DAVIS

DEPT OF DEFENSE CONTRACTORS (CONTINUED)

MARTIN MARIETTA DENVER AEROSPACE
ATTN: M POLZELLA
ATTN: R ANDERSON
ATTN: R KASE
ATTN: RESEARCH LIB

MARYLAND, UNIVERSITY OF
ATTN: H C LIN

MCDONNELL DOUGLAS CORP
ATTN: A P MUNIE
ATTN: D L DOHM
ATTN: M STITCH
ATTN: R L KLOSTER

MCDONNELL DOUGLAS CORP
ATTN: P ALBRECHT

MCDONNELL DOUGLAS CORP
ATTN: TECH LIB

MESSENGER, GEORGE C
ATTN: G MESSENGER

MISSION RESEARCH CORP
ATTN: C LONGMIRE

MISSION RESEARCH CORP
ATTN: R PEASE

MISSION RESEARCH CORP
ATTN: J LUBELL
ATTN: R CURRY
ATTN: W WARE

MISSION RESEARCH CORP, SAN DIEGO
ATTN: J RAYMOND
ATTN: V VAN LINT

MITRE CORPORATION
ATTN: M FITZGERALD

MOTOROLA, INC
ATTN: A CHRISTENSEN

MOTOROLA, INC
ATTN: C LUND
ATTN: L CLARK
ATTN: O EDWARDS

NATIONAL SEMICONDUCTOR CORP
ATTN: F C JONES

NEW MEXICO, UNIVERSITY OF
ATTN: DR NEAMEN

NORDEN SYSTEMS, INC
ATTN: N RIEDERMAN
ATTN: TECH LIBRARY

NORTHROP CORP
ATTN: A BAHRAMAN
ATTN: J SROUR
ATTN: Z SHANFIELD

NORTHROP CORP
ATTN: E KING
ATTN: S STEWART

PACIFIC-SIERRA RESEARCH CORP
ATTN: H BRODE, CHAIRMAN SAGE

PHYSICS INTERNATIONAL CO
ATTN: J SHEA

POWER CONVERSION TECHNOLOGY, INC
ATTN: V FARGO

R & D ASSOCIATES
ATTN: B LAMB
2 CYS ATTN: E MARTINELLI
2 CYS ATTN: G MESSENGER
2 CYS ATTN: G SAFONOV
ATTN: M GROVER
ATTN: W KARZAS

RAND CORP
ATTN: C CRAIN
ATTN: P DAVIS

RAND CORP
ATTN: B BENNETT

RAYTHEON CO
ATTN: G JOSHI
ATTN: J CICCIO

RAYTHEON CO
ATTN: A VAN DOREN
ATTN: H FLESCHER

RCA CORP
ATTN: G BRUCKER
ATTN: V MANCINO

RCA CORP
ATTN: R SMELTZER

RCA CORP
ATTN: E SCHMITT
ATTN: W ALLEN

RCA CORP
ATTN: E VAN KEUREN

DEPT OF DEFENSE CONTRACTORS (CONTINUED)

RENSSELAER POLYTECHNIC INSTITUTE
ATTN: R GUTMANN

RESEARCH TRIANGLE INSTITUTE
ATTN: M SIMONS

ROCKWELL INTERNATIONAL CORP
ATTN: A ROVELL
ATTN: GA50 TIC/L G GREEN
ATTN: J BELL
ATTN: J BURSON
ATTN: V DE MARTINO
ATTN: V STRAHAN

ROCKWELL INTERNATIONAL CORP
ATTN: TIC AJ01

ROCKWELL INTERNATIONAL CORP
ATTN: L W PINKSTON
ATTN: TIC 124-203

ROCKWELL INTERNATIONAL CORP
ATTN: T YATES
ATTN: TIC BA08

ROCKWELL INTERNATIONAL CORP
ATTN: J BURSON

SCIENCE APPLICATIONS INTL CORP
ATTN: D LONG
ATTN: D MILLWARD
ATTN: D STROBEL
ATTN: L SCOTT
ATTN: R FITZWILSON
ATTN: R J BEYSTER
ATTN: V ORPHAN
ATTN: V VERBINSKI

SCIENCE APPLICATIONS INTL CORP
ATTN: J SPRATT

SCIENCE APPLICATIONS INTL CORP
ATTN: W CHADSEY

SCIENCE APPLICATIONS INTL CORP
ATTN: P A ZIELIE

SCIENTIFIC RESEARCH ASSOC, INC
ATTN: H GRUBIN

SINGER CO
ATTN: R SPIENGEL
ATTN: TECH INFO CNTR

SPERRY CORP
ATTN: J INDA

SPERRY CORP
ATTN: P MARROFFINO

SRI INTERNATIONAL
ATTN: A PADGETT

SUNDSTRAND CORP
ATTN: C WHITE

SYSTEM DEVELOPMENT CORP
ATTN: PRODUCT EVAL LAB

SYSTRON-DONNER CORP
ATTN: J RAY

TELEDYNE BROWN ENGINEERING
ATTN: G R EZELL

TELEDYNE SYSTEMS CO
ATTN: R SUHRKE

TEXAS INSTRUMENTS, INC
ATTN: E JEFFREY
ATTN: F POBLENZ
ATTN: J SALZMAN
ATTN: T CHEEK

TRW ELECTRONICS & DEFENSE SECTOR
ATTN: A WITTELES
ATTN: D CLEMENT
ATTN: F FRIEDT
ATTN: H HOLLOWAY
ATTN: M S ASH
2 CYS ATTN: O ADAMS
ATTN: P GUILFOYLE
ATTN: P R REID
2 CYS ATTN: R PLEBUCH, HARD & SURV LAB
ATTN: R VON HATTEN
ATTN: TECH INFO CTR, DOC ACQ
ATTN: W B ADELMAN
ATTN: W ROWAN
ATTN: W WILLIS

TRW ELECTRONICS & DEFENSE SECTOR
ATTN: C BLASNEK
ATTN: F FAY
ATTN: J GORMAN

VISIDYNE, INC
ATTN: C H HUMPHREY
ATTN: W P REIDY

WESTINGHOUSE ELECTRIC CORP
ATTN: D GRIMES
ATTN: H KALAPACA
ATTN: R CRICCHI

WESTINGHOUSE ELECTRIC CORP
ATTN: S WOOD

END

3-87

DTIC